

Path planning with uncertainty: a set membership approach

Nicola Ceccarelli, Mauro Di Marco, Andrea Garulli,
Antonio Giannitrapani, Antonio Vicino*

Abstract

The paper addresses the path planning problem in a set theoretic framework. The considered scenario is that of a mobile robot exploiting range and bearing measurements with respect to known landmarks to localize itself. By assuming unknown but bounded measurement noise, set membership localization techniques are used to estimate the uncertainty of each robot pose within the considered environment. The path planning problem is formulated and solved, with the aim of minimizing the total uncertainty associated to the travelled path. Practical issues such as limited sensory range and obstacle avoidance are taken into account. The proposed technique is validated via numerical simulations.

Keywords: Path planning; navigation uncertainty; set membership; localization; landmarks.

1 INTRODUCTION

The *set membership* estimation paradigm has been introduced to cope with uncertainty in a deterministic framework and it has been successfully applied in a wide spectrum of application fields in which statistical assumptions on the uncertainty sources are unreliable or difficult to be validated (see e.g. [1, 2] and references therein). Mobile robotics has also benefited from a number of contributions in the set membership framework. The problem of localizing a mobile robot within a known environment has been addressed in several different scenarios [3, 4, 5, 6, 7]. More challenging problems, such as simultaneous localization and map building (SLAM) [8, 9] and collaborative localization for a team of mobile robots [10], have also been addressed. The main idea underlying these

*The authors are with the Dipartimento di Ingegneria dell'Informazione, Via Roma, 56 - 53100 Siena, Italy. Email: giannitrapani@dii.unisi.it.

approaches is that the uncertainty sources (disturbances affecting the robot motion model, measurement noise, etc.) are modelled as *unknown-but-bounded* (UBB) signals. Under this hypothesis, the problem can be cast in terms of *feasible sets*, defined as those sets containing all the admissible robot poses (positions and orientations) compatible with the whole available information and the bounds on the error. The techniques proposed in the literature basically differ for the considered motion and sensory models, and for the way feasible sets are computed or approximated.

The navigation system of a fully autonomous mobile robot has to integrate several tasks, such as sensing, environmental mapping, localization and path planning. Motion planning has been recognized as a key problem in mobile robotics for some time [11]. A large variety of solutions have been proposed, which proved to be effective in practice (see [12] for a comprehensive review). However, being the problem computationally intensive, uncertainty and disturbances have been often neglected in the path planning phase, i.e., the robot position is usually assumed to be known exactly. Nevertheless, in recent years the number of contributions addressing path planning with uncertainty is steadily increasing. The objective of these works is the computation of safe paths, ensuring that the goal is reached in spite of the uncertainty affecting the robot pose and/or the environment map. Clearly, the path planner must be designed in order to cope with the adopted uncertainty representation.

Similarly to what happens for other tasks, such as localization or mapping, the approaches proposed in the literature can be classified according to the paradigm adopted for modelling uncertainty. Probabilistic uncertainty representations have been considered by several authors (see e.g. [13, 14, 15, 16]). In [17] a mobile robot performs measurements with respect to landmarks to localize itself, and the pose uncertainty estimated by an extended Kalman filter is exploited to design safe paths. Path planning based on deterministic uncertainty representations has also been investigated. There is an extensive literature on path planners using sets to model uncertainties (see [18] and references therein), but in most of these works uncertainty is not related to localization errors arising from sensing and motion disturbances. One of the first papers explicitly accounting for uncertainty both in the motion model and in the sensing process is [19]. In [20], an ellipsoidal set membership localization technique is combined with a path planner based on evolutionary computation. The computed feasible sets are used to ensure safe obstacle avoidance, rather than to minimize the overall uncertainty along the path.

In this paper, we focus on a set theoretic approach to the path planning problem, in order to take into account the localization uncertainty associated to the selected paths. In particular, the problem of finding a trajectory minimizing the overall position uncertainty along the path, is

tackled. This is motivated by applications in which it is crucial to localize the robot as precisely as possible along the whole path and not only in the final target, typical examples being the exploration of unknown environments or the accomplishments of several tasks requiring a prescribed precision along the travelled path. The considered scenario is that of a mobile robot performing range and bearing measurements with respect to known landmarks. UBB measurements errors are assumed. The set membership localization technique proposed in [8] is employed to estimate the uncertainty set associated to each robot pose. Then, the path planning problem is formulated as an optimal control problem, whose objective function is the total position uncertainty of the path travelled from the starting point to the assigned goal. The proposed technique has to be intended as a high level planner whose output is a sequence of way points feeding a low-level trajectory generation and tracking module. Obstacle avoidance and limited sensory range are taken into account in the formulation of the optimization problem. A preliminary version of this work has been presented in [21].

The paper is organized as follows. Section 2 describes the set theoretic uncertainty representation and the related localization technique. Section 3 introduces the path planning problem in the set theoretic framework and formulates the related optimization problems. Section 4 presents several simulation results, while some concluding remarks are given in Section 5.

2 SET THEORETIC LOCALIZATION

Let us consider a robot navigating in a 2D environment, whose pose at time k is denoted by

$$p(k) = [x(k) \ y(k) \ \theta(k)]' \in \mathcal{Q},$$

with $\mathcal{Q} \triangleq \mathbb{R}^2 \times [-\pi, \pi]$ being the set of all possible robot configurations. The coordinates $(x(k), y(k))$ represent the position of the vehicle, while $\theta(k)$ denotes its orientation (view direction), with respect to the positive x -axis. It is assumed that a map of the environment is available, in terms of n static pointwise landmarks, having known positions:

$$l_i = [x_{l_i} \ y_{l_i}]', \quad i = 1, \dots, n.$$

The robot is supposed to be equipped with exteroceptive sensors, measuring m quantities $y_i(k) \in \mathbb{R}^m$ related to each landmark l_i

$$y_i(k) = h(p(k), l_i) + v_i(k). \quad (1)$$

In (1), the signal $v_i(k) \in \mathbb{R}^m$ denotes the measurement noise and is supposed to be norm-bounded

$$\|v_i(k)\|_{\infty}^{\epsilon_v} \leq 1, \quad (2)$$

where, for a vector $w = [w_1, \dots, w_n]'$ with positive entries, the weighted ∞ norm $\|x\|_\infty^w$ is defined as $\|x\|_\infty^w \triangleq \max_i |x_i/w_i|$. The bounded error assumption (2) allows one to define for each measurement y_i a set

$$\mathcal{M}_i(p(k)) = \{p(k) \in \mathcal{Q} : \|y_i(k) - h(p(k), l_i)\|_\infty^{\epsilon_v} \leq 1\}. \quad (3)$$

containing all robot poses compatible with the i -th measurement readings (1) and the corresponding noise bound (2). In a set theoretic framework, data fusion is obtained via set intersection. Hence, supposing that at time k the robot performs measurements with respect to the n landmarks, its pose is constrained to lie in the *feasible set*

$$\mathcal{M}(p(k)) = \bigcap_{i=1}^n \mathcal{M}_i(p(k)). \quad (4)$$

Notice that, if the measurement noise is within the bound (2), the set $\mathcal{M}(p(k))$ is not empty. On the contrary, an empty intersection in (4) implies that at least one of the constraints in (2) has been violated. An appealing property of the set theoretic formulation is that, as long as the errors verify the boundedness assumption, the actual robot pose $p(k)$ is guaranteed to belong to the set $\mathcal{M}(p(k))$ (*feasibility property*), regardless of the statistical nature of the noise. Such a property turns out to be especially useful whenever “certified” estimates are needed, e.g. in order to plan safe paths. Moreover, a measure of the quality of the set-valued estimates is given by the size of the corresponding feasible sets.

In this paper, the robot is supposed to have on-board sensors like laser range finders or stereo vision systems, providing *range and bearing* measurements with respect to the landmarks (see Figure 1). In this case, the measurement equations (1) take on the form $y_i(k) = [D_i(k) \ A_i(k)]'$, where

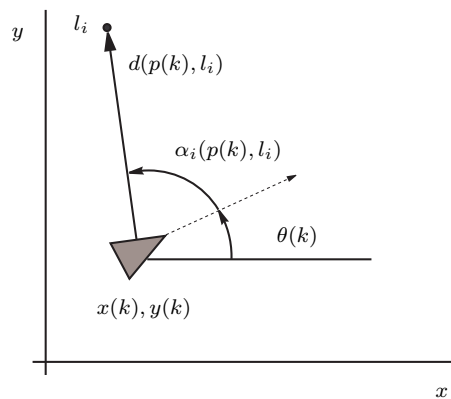


Figure 1: Range and bearing measurement with respect to the i -th landmark.

$$\begin{aligned} D_i(k) &= d(p(k), l_i) + v_{d_i}(k) \\ A_i(k) &= \alpha(p(k), l_i) + v_{\alpha_i}(k) \end{aligned} \quad i = 1, \dots, n. \quad (5)$$

In equations (5), $D_i(k)$ and $A_i(k)$ are the actual sensor readings and $v_{d_i}(k)$, $v_{\alpha_i}(k)$ model noise affecting the distance and angular measurements, defined as

$$d(p(k), l_i) \triangleq \sqrt{(x(k) - x_{l_i})^2 + (y(k) - y_{l_i})^2}, \quad (6)$$

$$\alpha(p(k), l_i) \triangleq \text{atan}_2(y_{l_i} - y(k), x_{l_i} - x(k)) - \theta(k). \quad (7)$$

In (7), $\text{atan}_2(\cdot, \cdot)$ denotes the four quadrant inverse tangent. The assumption (2) of bounded measurement noise can be explicitly written as

$$|v_{d_i}(k)| \leq \epsilon^{v_d}, \quad (8)$$

$$|v_{\alpha_i}(k)| \leq \epsilon^{v_\alpha}, \quad (9)$$

with ϵ^{v_d} and ϵ^{v_α} denoting known (possibly time-varying) positive scalars. Consequently, the sets $\mathcal{M}_i(p(k))$ in (3) associated to each measurement pair $D_i(k)$, $A_i(k)$ become

$$\mathcal{M}_i(p(k)) = \{p(k) \in \mathcal{Q} : |D_i(k) - d(p(k), l_i)| \leq \epsilon^{v_d} \text{ and } |A_i(k) - \alpha(p(k), l_i)| \leq \epsilon^{v_\alpha}\}.$$

The exact solution to the set theoretic localization problem involves the computation of the feasible set $\mathcal{M}(p(k))$ in (4). Unfortunately, this set turns out to be the intersection of nonlinear, nonconvex 3D sets, whose shape can be very complex. Two major drawbacks prevent from computing its exact expression. As far as real-time applications are concerned, the computation required by (4) may be too expensive. Moreover, as new measurements are processed, the shape of the feasible pose set can become arbitrarily complex, so that finding analytical expressions is a very hard problem. For these reasons, suboptimal solutions, trying to reduce the computational burden, while at the same time preserving the essential features of the set-valued estimates, have been devised. For instance, in [8] outer approximations of the feasible sets via simple structure regions have been proposed. It has been shown that, at the expense of some conservativeness, it is possible to devise efficient recursive algorithms able to compute guaranteed set estimates.

To illustrate the main idea, let us first suppose that the robot orientation $\theta(k)$ is known. It is easily verified that the projection on the xy -plane of each set $\mathcal{M}_i(p(k))$ corresponds to a ring sector $\mathcal{C}_i(p(k))$, whose radial and angular semi-amplitude are given by ϵ^{v_α} and ϵ^{v_d} , respectively (see Figure 2(a)). Then, all the admissible robot positions at time k , according to the error bounds and the measurements $D_i(k)$, $A_i(k)$, are constrained into the set

$$\mathcal{C}(p(k)) = \bigcap_{i=1}^n \mathcal{C}_i(p(k)). \quad (10)$$

The goal is to bound the set $\mathcal{C}(p(k))$ by the minimum area set belonging to a class of simple regions.

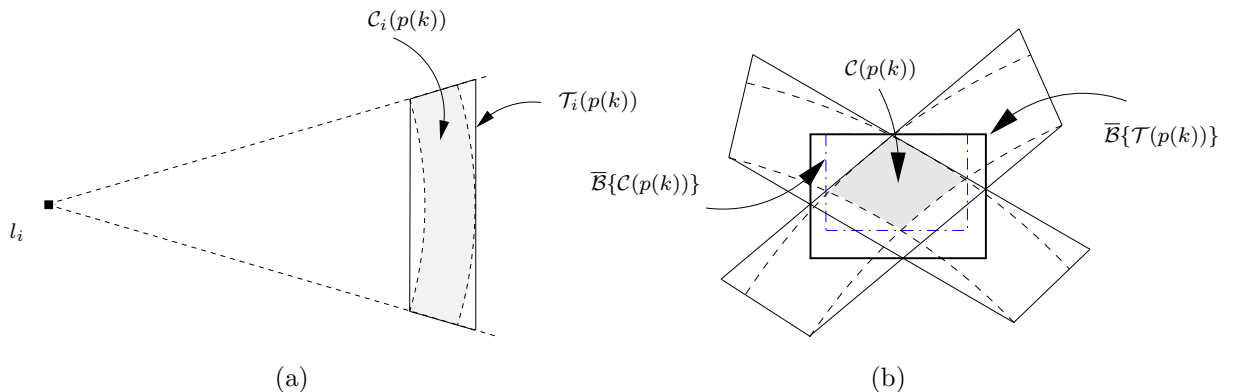


Figure 2: (a) Trapezoidal approximation of a ring sector. (b) Outer approximation of the exact feasible position set $\mathcal{C}(p(k))$ (dashed region) related to two landmarks.

In this paper, axis-aligned boxes will be used. To this purpose, let us denote by $\overline{\mathcal{B}}\{\mathcal{Z}\}$, the minimum area box containing the set \mathcal{Z} . Notice that the set in (10) is still nonconvex. Hence, to further simplify the computation, rather than finding the smallest box containing $\mathcal{C}(p(k))$, we look for the minimum area box outbounding the set $\mathcal{T}(p(k))$, defined as

$$\mathcal{T}(p(k)) = \bigcap_{i=1}^n \mathcal{T}_i(p(k)), \quad (11)$$

where each $\mathcal{T}_i(p(k))$ denotes the minimum area trapezoid containing each ring sector $\mathcal{C}_i(p(k))$, as shown in Figure 2(a). Notice that $\mathcal{T}_i(p(k))$ can be analytically computed, from the landmark location l_i , the sensor readings $D_i(k), A_i(k)$ and the error bounds (8)-(9). With this choice, the problem becomes the computation of

$$\mathcal{B}(p(k)) = \overline{\mathcal{B}}\{\mathcal{T}(p(k))\}, \quad (12)$$

which in turns boils down to the solution of four linear programming problems. It is worth remarking that the set $\mathcal{B}(p(k))$ contains, by construction, the true robot position (see Figure 2(b)).

To take into account also the uncertainty affecting the vehicle orientation estimates, the above procedure has to be slightly modified. At each time k , an interval estimate of the actual robot orientation can be derived, from a simple geometrical reasoning. Such uncertainty can be suitably taken into account by enlarging the angular amplitude of each ring sector, by a quantity equal to the width of the orientation uncertainty interval.

The framework described above can easily incorporate also a dynamic model of the robot, in which uncertainties are modelled as UBB disturbances. In this case, the set estimate $\mathcal{B}(k)$ can be

recursively updated by using prediction-correction schemes analogous to that adopted in EKF. The interested reader is referred to [8] for a detailed treatment of set membership localization algorithms.

3 SET THEORETIC PATH PLANNING

In this section, the problem of computing minimum uncertainty paths is addressed, exploiting the set theoretic localization framework illustrated in Section 2. First, the problem is cast as an optimal control problem for generic robot motion models and measurement equations. Then, the problem is specialized to meet the specific scenario considered in this paper. The resulting optimization problem is later relaxed in order to reduce its computational burden. This is achieved by modifying the cost function to make it independent from the robot orientation, and by replacing the exact feasible sets with approximating boxes, like it has been done in Section 2.

Consider a robot with initial pose p_0 and whose target is to reach a pose p_T , after T moves. The objective is to plan a path $\mathcal{P} = [p(0), p(1), \dots, p(T)]$, such that the average uncertainty associated to the path is minimized. Let

$$p(k+1) = f(p(k), u(k)) \quad (13)$$

be a dynamic model of the robot pose, where $u(k) \in \mathbb{R}^p$ is the control input and $p(k)$ represents the state. Since the objective is to find a path minimizing the localization uncertainty, let us choose as cost function the volume $V[\mathcal{M}(p(k))]$ of the feasible set $\mathcal{M}(p(k))$ defined in (4). Now, the path planning problem can be cast as the optimal control problem

$$\begin{aligned} & \min_{u(0), \dots, u(T-1)} \frac{1}{T} \sum_{k=0}^{T-1} V[\mathcal{M}(p(k))] \\ & \text{s.t.} \\ & p(k+1) = f(p(k), u(k)), \quad k = 0, \dots, T-1, \\ & \|u(k)\|_{\infty}^b \leq 1, \quad k = 0, \dots, T-1, \\ & p(0) = p_0, \quad p(T) = p_T. \end{aligned} \quad (14)$$

In (14), the weight vector $b = [b_1, \dots, b_m]'$ contains the bounds on each component of the control input $u(k)$, i.e. $|u_i(k)| \leq b_i$. The complexity of the previous optimization problem depends on: i) the kind of measurements available (which define the shape of the set $\mathcal{M}(p(k))$); ii) the robot motion model (13). For instance, nonlinear robot dynamics result in nonlinear equality constraints in (14). Since our objective is to find an optimal sequence of way points in the configuration space that the planner provides to the low-level motion control unit, a simple robot motion model can be adopted

in place of (13)

$$p(k+1) = p(k) + u(k) \quad (15)$$

where the control input $u(k) = [u_x(k), u_y(k), u_\theta(k)]'$ now represents the x -, y - and θ - displacement between two consecutive way points. Hence, the constraints on the input become simply constraints on the maximum pose variation at each move, i.e.

$$|u_x(k)| \leq b_x, \quad |u_y(k)| \leq b_y, \quad |u_\theta(k)| \leq b_\theta, \quad (16)$$

where $b_x > 0$ and $b_y > 0$. The bound b_θ on the orientation is set to π . This basically means that bounds on the maximum rotation in a sample interval are neglected. It is assumed that the time step for a single move is such that the robot succeeds to perform the required rotation during each move, which is in agreement with the considered planning setup. According to the assumptions (15)-(16), the optimal control problem (14) reduces to

$$\begin{aligned} & \min_{u(0), \dots, u(T-1)} \frac{1}{T} \sum_{k=0}^{T-1} V[\mathcal{M}(p(k))] \\ & \text{s.t.} \\ & p(k+1) = p(k) + u(k), \quad k = 0, \dots, T-1, \\ & |u_x(k)| \leq b_x, \quad k = 0, \dots, T-1, \\ & |u_y(k)| \leq b_y, \quad k = 0, \dots, T-1, \\ & p(0) = p_0, \quad p(T) = p_T. \end{aligned} \quad (17)$$

The optimization problem (17) is still hard to solve, due to the complexity of the cost function. For instance, if range and bearing measurements are used, $\mathcal{M}(p(k))$ are nonlinear, nonconvex sets. Moreover, additional difficulties make the solution of (17) even more challenging. In particular:

- a) the set $\mathcal{M}(k)$ is a function of the sensor readings $D_i(k), A_i(k)$, which in turn depend on the actual realization of measurement noises;
- b) the size of $\mathcal{M}(k)$ does not depend on the robot orientation $\theta(k)$ if the visibility range is unlimited and all landmarks can be seen from any robot pose; in the more realistic situation of limited field of view, $V[\mathcal{M}(k)]$ depends on which landmarks fall in the robot field of view.

Problem a) can be faced in a worst-case approach, by maximizing $V[\mathcal{M}(k)]$ over all possible noise realizations. However, this would lead to an untractable high-dimensional min-max optimization problem. A more viable approach is that of neglecting the noise realizations in the planning phase,

which amounts to consider measurements $D_i(k), A_i(k)$ produced by a zero noise realization. Notice that this is generally an unfavorable case in set theoretic localization, where the maximum uncertainty reduction is usually achieved when the noise sequence takes values on the boundary as often as possible.

In order to cope with problem b), a suitable partition of the orientation interval is introduced next. As it will become clear in the following, this will also lead to a useful simplification of the cost function in (17).

3.1 Limited visibility

In a real-world scenario, sensors usually feature limited field of view. For example, a mobile robot using a laser rangefinder can only detect landmarks lying inside a given circular sector, which is determined by the maximum range and bearing that the sensor can measure.

In this work, we assume that a robot can see all the landmarks l_i such that $|\alpha(p(k), l_i)| \leq \bar{\alpha}$ and $d(p(k), l_i) \leq \bar{d}$, where $\bar{\alpha}$ and \bar{d} denotes the angular and linear visibility, respectively. This assumption implies that, given a position $z = [x, y]'$, the robot perceives different sets of landmarks depending on both its orientation θ and its visibility region given by $\bar{\alpha}$ and \bar{d} . Therefore, the intersections in (4), (10) and (11) do not involve all the landmarks, but only those that are actually seen from the current pose $p(k)$.

In order to establish which landmarks are seen from a given pose, we look for a partition of the orientation interval $[-\pi, \pi]$ into subsets h_i , such that each subset h_i is associated to a unique set of visible landmarks from the position z and *for all* orientations $\theta \in h_i$. For a fixed position z , let us introduce the set

$$\tau_h = \{l_j : |\alpha(p, l_j)| \leq \bar{\alpha} \text{ and } d(p(k), l_j) \leq \bar{d} \quad \forall p = [x, y, \theta] \text{ with } \theta \in h\} \quad (18)$$

which represents the set of visible landmarks, from position z and orientation $\theta \in h$, with $h \subseteq [-\pi, \pi]$.

Then, the sought partition of $[-\pi, \pi]$ is given by

$$\begin{aligned} \mathcal{H}(z) &= \{h_i \subseteq [-\pi, \pi] : \\ &\quad \bigcup h_i \equiv [-\pi, \pi] \\ &\quad h_i \cap h_j = \emptyset \quad \forall i \neq j \\ &\quad \tau_{h_i} \neq \tau_{h_j} \quad \forall i \neq j \\ &\quad \tau_a \equiv \tau_{h_i} \quad \forall a \subseteq h_i \}. \end{aligned} \quad (19)$$

Notice that $\mathcal{H}(z)$ is a partition of the interval $[-\pi, \pi]$ into disjoint sets, such that the landmarks perceived by any couple of orientations $\theta_i \in h_i$ and $\theta_j \in h_j$ are different if $h_i \neq h_j$. Moreover, the

landmarks perceived is the same in every subset of h_i . This makes the partition defined by (18)-(19) unique.

To clarify how the partition $\mathcal{H}(z)$ is constructed, let us consider the example depicted in Figure 3, concerning a 4 landmarks scenario with unbounded linear visibility ($\bar{d} = \infty$) and limited angular visibility ($\bar{\alpha} = \frac{\pi}{2}$). In this case, one gets the partition $\mathcal{H}(z) = \{h_1, h_2, h_3, h_4, h_5, h_6\}$. Table 1 reports the sets of visible landmarks τ_{h_j} , from pose $p = [x, y, \theta]$ with $\theta \in h_j$.

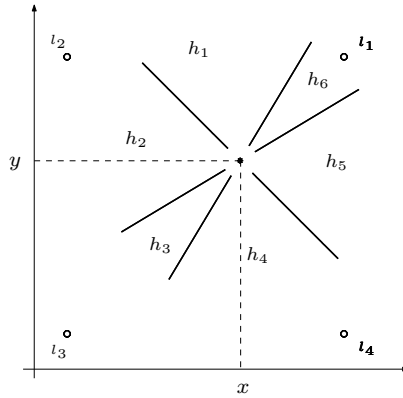


Figure 3: Example of orientation partition: asterisk denotes the robot position $z = [x, y]'$, circles represent landmark positions, solid lines bound the angular subsets h_i .

Table 1: Sets of visible landmarks τ_{h_i} for the example in Figure 3.

τ_{h_1}	l_1, l_2
τ_{h_2}	l_2, l_3
τ_{h_3}	l_2, l_3, l_4
τ_{h_4}	l_3, l_4
τ_{h_5}	l_1, l_4
τ_{h_6}	l_1

3.2 A simplified optimization problem

The previous discussion suggests that the problem of choosing the robot orientation along the path can be simplified into that of selecting a suitable orientation subset h_j . In fact, given a robot

orientation $\theta(k) \in h_j$, the feasible set (4) associated to the robot pose $p(k)$ becomes

$$\mathcal{M}^{(j)}(p(k)) = \bigcap_{l_i \in \tau_{h_j}} \mathcal{M}_i(p(k)) \quad (20)$$

where $h_j \in \mathcal{H}(z)$ is an element of the partition (19). Clearly, the size of $\mathcal{M}^{(j)}(p(k))$ in (20) depends on τ_{h_j} , and hence on the partition subset h_j in which the robot orientation lies, but it does not depend on the exact value $\theta(k)$ of the orientation itself. For this reason, one can get rid of the dependence on $\theta(k)$ in the cost function (17), by choosing the subset h_j for which the size of the feasible set $\mathcal{M}^{(j)}(p(k))$ in (20) is minimum. This amounts to consider for each position $z(k)$ the cost function

$$\mathcal{J}(z(k)) = \min_{h_j \in \mathcal{H}(z(k))} V \left[\mathcal{M}^{(j)}(p(k)) \right]. \quad (21)$$

If $V[\mathcal{M}(p(k))]$ in (17) is replaced by $\mathcal{J}(z(k))$, the number of free variables in the optimization problem is reduced from $3T$ to $2T$. However, the cost function (21) is still very difficult to compute, since the $\mathcal{M}^{(j)}(p(k))$ are nonlinear, nonconvex 3D sets.

A further simplification is achieved by considering only the position uncertainty and exploiting the set approximation introduced in Section 2. In particular, the feasible set approximation worked out in (11)-(12) becomes

$$\mathcal{B}^{(j)}(z(k)) = \bar{\mathcal{B}} \left\{ \bigcap_{l_i \in \tau_{h_j}} \mathcal{T}_i(p(k)) \right\}.$$

Hence, one can replace $\mathcal{J}(z(k))$ with the new cost

$$\mathcal{J}_2(z(k)) = \min_{h_j \in \mathcal{H}(z(k))} A \left[\mathcal{B}^{(j)}(z(k)) \right]. \quad (22)$$

where $A[\cdot]$ denotes the area of the set within square brackets. Notice that, according to the discussion in Section 2, in (22) the uncertainty in robot orientation is neglected: this means that in the planning phase one assumes to know exactly the orientation of the robot when computing the size of the (approximate) feasible position set.

At this point, the optimal control problem (17) boils down to the following optimization problem

$$\begin{aligned} & \min_{w(0), \dots, w(T-1)} \frac{1}{T} \sum_{k=0}^{T-1} \mathcal{J}_2(z(k)) \\ & \text{s.t.} \\ & z(k+1) = z(k) + w(k), \quad k = 0, \dots, T-1, \\ & |w_x(k)| \leq b_x, \quad k = 0, \dots, T-1, \\ & |w_y(k)| \leq b_y, \quad k = 0, \dots, T-1, \\ & z(0) = \Pi p_0, \quad z(T) = \Pi p_T. \end{aligned} \quad (23)$$

where $\Pi = [I_2 \ 0_{2 \times 1}]$ and $w(k) = [w_x(k), w_y(k)]' = \Pi u(k)$.

The optimization problem (23) is in general non convex. In this paper, the problem is solved by applying Sequential Quadratic Programming (SQP). The solution $w^*(0), \dots, w^*(T-1)$ of (23) provides a sequence of positions $z^*(1), \dots, z^*(T)$. To solve completely the path planning problem one has to specify the orientations $\theta^*(k)$ associated to the positions $z^*(k)$. In order to minimize the uncertainty along the path one should consider the set of orientations for which the minimum in (22) is achieved, i.e.

$$h_{j^*}(k) = \arg \min_{h_j \in \mathcal{H}(z^*(k))} A \left[\mathcal{B}^{(j)}(z(k)) \right]. \quad (24)$$

Any value within $h_{j^*}(k)$ can be selected as the robot orientation $\theta^*(k)$ at the k -th step of the computed path. In this paper, the orientations $\theta^*(k)$ are chosen as the centers of the intervals $h_{j^*}(k)$ defined in (24).

3.3 Obstacle avoidance

In real-world applications, the path planner must also deal with the presence of obstacles. In case of stationary obstacles with known position, one of the most popular techniques for tackling this problem is the potential field approach [12], where artificial potential functions are generated according to the shape and the location of the obstacles. Once such functions are generated, they can be combined with the cost function in (22), in order to produce a new cost to be minimized in (23). A possible choice, is to replace $\mathcal{J}_2(z)$ in (23) by

$$\mathcal{J}_2(z) + \rho \mathcal{O}(z) \quad (25)$$

where $\mathcal{O}(z)$ is the artificial potential function associated to the obstacles, and ρ is a suitable weighting coefficient. Clearly, the resulting cost function accounts both for uncertainty along the path and for the presence of obstacles in the scene. On the other hand the use of potential functions usually complicates the solution of (23) increasing the occurrence of local minima, which represent a well-known drawback of such approaches (e.g., see [22]).

4 SIMULATION RESULTS

In this section, simulation results concerning the proposed path planning strategy are presented. The computed path has been used to simulate a mobile robot navigation, during which the localization algorithm sketched in Section 2 is applied. Different path choices are compared in terms of localization accuracy.

The first set of simulations has been carried out in a scenario involving 4 landmarks (scenario A). The aim is to solve the path planning problem (23) with the constraints $p_0 = [-3 \ -4 \ 0]'$, $p_T = [5 \ 4 \ \pi]$, $b_x = b_y = 1$, and $T = 14$. The cost function $\mathcal{J}_2(z)$ in (22) has been computed via the set approximation techniques described in Section 2, assuming the noise bounds in (8)-(9) given by:

$$\begin{aligned}\epsilon^{v_d} &= 0.1 \text{ (m)}, \\ \epsilon^{v_\alpha} &= 5 \text{ (deg)},\end{aligned}$$

The on-board sensor is supposed to have unbounded linear visibility ($\bar{d} = \infty$) and limited angular visibility $\bar{\alpha} = \pi/2$. The resulting $\mathcal{J}_2(z)$ for this scenario is shown in Figure 4(a), while the corresponding orientations are reported in Figure 4(b). The computed path is shown in Figure 4(c).

Figure 5 shows the cost function and the computed path for the same scenario, in which two rectangular obstacles have been added. It is supposed that the obstacles do not prevent detection of landmarks (this is the case, e.g., of radio frequency beacons). The cost function has been generated according to equation (25). The resulting path has been analyzed by simulating the motion of a mobile robot performing self-localization along the path. The localization algorithm combines the set approximation techniques outlined in Section 2 for processing range and bearing measurements, with a simple kinematic model for robot motion. In particular, it is assumed that the robot pose evolves as

$$p(k+1) = p(k) + u(k) + w(k) \quad (26)$$

where $u(k)$ represents translation and rotation measurements from odometric sensors, and $w(k)$ models the errors affecting $u(k)$. Also the disturbance $w(k)$ are supposed to be UBB. Specifically, bounds on translation errors are set to 10% of the x -, y -displacement, respectively, while bounds on rotation errors are set to 5% of the variation of θ . At each move, the set of feasible robot poses is enlarged according to the model (26); each time measurements are performed, such a set is reduced by intersecting it with the set $\mathcal{B}(k)$ in (12). A detailed description of the dynamic localization algorithm can be found in [8].

The performance of the localization algorithm has been compared for three different paths:

t_{opt} : the path obtained by solving problem (23);

t_{d_1} : the direct path joining p_0 to p_T , where the orientations are chosen as the center of the interval h_{j^*} in (24);

t_{d_2} : the direct path joining p_0 to p_T , where the orientation is kept equal to the one pointing from $z(0)$ to $z(T)$.

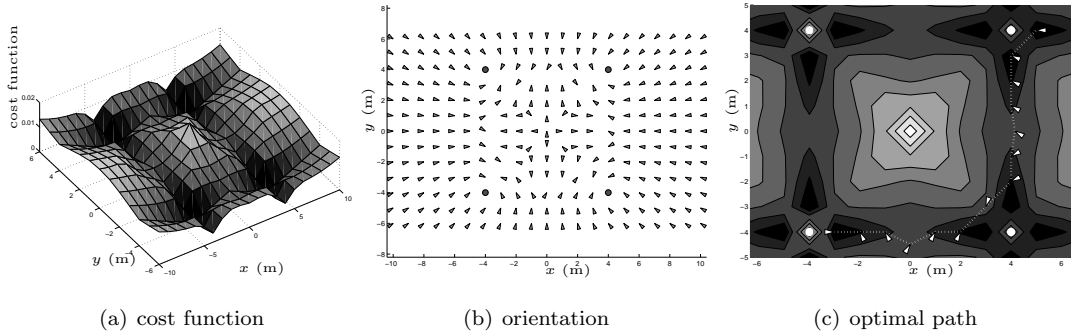


Figure 4: Scenario A: (a) cost function (22), (b) associated orientations, (c) path calculated by solving the optimization problem (23). White triangles represent the selected robot poses, white circles denote the landmarks. Contour lines of the cost function are reported in background.

It is worth remarking that, while the path planning is performed assuming zero measurement noise realizations, in the simulations the disturbance signals v_{d_i} , v_{α_i} , w are generated as independent uniformly distributed random variables within the given bounds. In each simulation run, the uncertainty affecting the robot pose is computed in terms of boxes containing the robot position $z(k)$ and intervals containing the robot orientation $\theta(k)$, for each k . Simulation results are averaged over 100 runs with different noise realizations. Figure 6 reports the result of typical runs for the considered paths t_{opt} , t_{d_1} and t_{d_2} . It can be noticed that the uncertainty on the robot position is smaller along the path t_{opt} , as expected. The comparison between the two direct paths t_{d_1} and t_{d_2} in Figures 6(b) and 6(c) confirms that the choice of orientations along the path plays an important role in uncertainty reduction. Average uncertainties on position and orientation are shown in Figure 7. It can be noticed that, although the uncertainty values are similar at the endpoints of the path, the overall uncertainty is significantly smaller along the selected path t_{opt} .

A second set of simulations has been performed in an environment with 7 landmarks and two obstacles (scenario B). In this test, the sensor is supposed to have both linear and angular limited visibility, with $\bar{d} = 3$ and $\bar{\alpha} = \pi/2$. The number of steps is $T = 15$ and the maximum displacement during each robot move is $b_x = b_y = 2$. The other parameters are the same as before. The resulting path, superimposed to the contour plot of the cost function, is shown in Figure 8. In this case, given the limited range of the sensor, there exist regions of the environment where the robot does not perceive any landmark (see the homogeneous gray area in Figure 8). Since in these locations the robot is not able to localize itself, the potential $\mathcal{J}_2(z)$ in (23) is very high and the planner correctly attempts to avoid these zones. The comparison of the localization uncertainty along the optimal path t_{opt} and the direct path with optimal orientation t_{d_1} is shown in Figure 9. As before, the robot

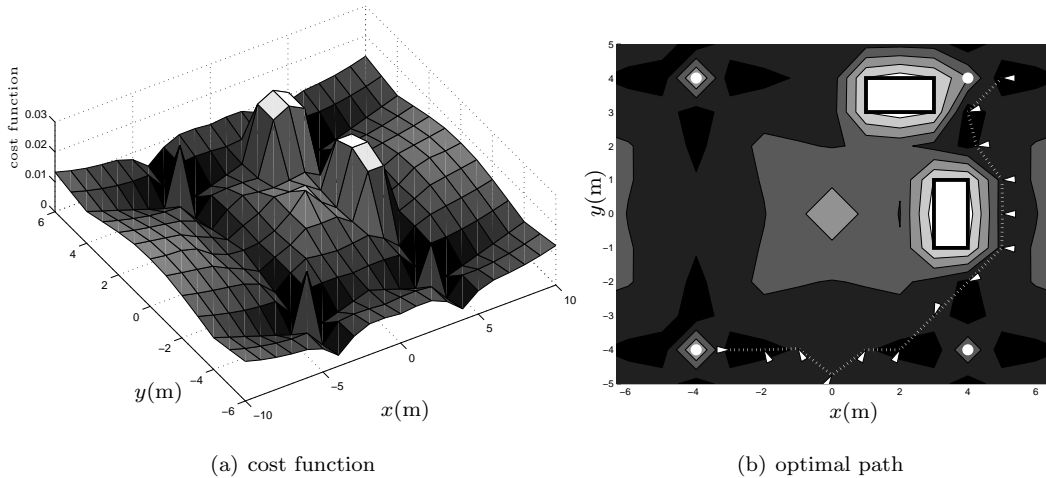


Figure 5: Scenario A with obstacles: (a) cost function (25), (b) path calculated by solving the optimization problem (23) with the cost function (25)

performs self-localization using the motion model (26). The statistics of the process disturbance $w(k)$ and of the measurement noise v_{d_i}, v_{α_i} are equal to those of the previous scenario. In this case, due to the limited linear visibility of the sensor, the improvement in terms of localization accuracy yielded by an optimal planning is even more evident than before.

Finally, several simulations have been done in environments populated with a larger number of landmarks. Scenario C refers to the case of 28 landmarks, spread over an area of about $800 m^2$ (see Figure 10). Such a configuration aims at modelling an outdoor environment with pointwise landmarks (e.g., trees, corners of buildings, etc.) mostly grouped in three different regions. This kind of environments are commonly found in practice and can be considered a sort of testbed for localization and mapping purposes (see, e.g., the well known Victoria Park data set introduced in [23]). The parameters used in the simulations are equal to those adopted in scenario B, except for the maximum displacement $b_x = b_y = 4$ and the linear visibility of the sensor $\bar{d} = 7$. In this case, the optimal path t_{opt} passes through the landmark clusters, which correspond to highly informative regions for localization purposes. On the contrary, the linear path t_{d_1} , connecting starting and ending point, lies in an area of the environment where only few landmarks are visible (if any), resulting in poor localization accuracy. This phenomenon is confirmed by the comparison of the localization uncertainty along the two paths, as shown in Figure 11.

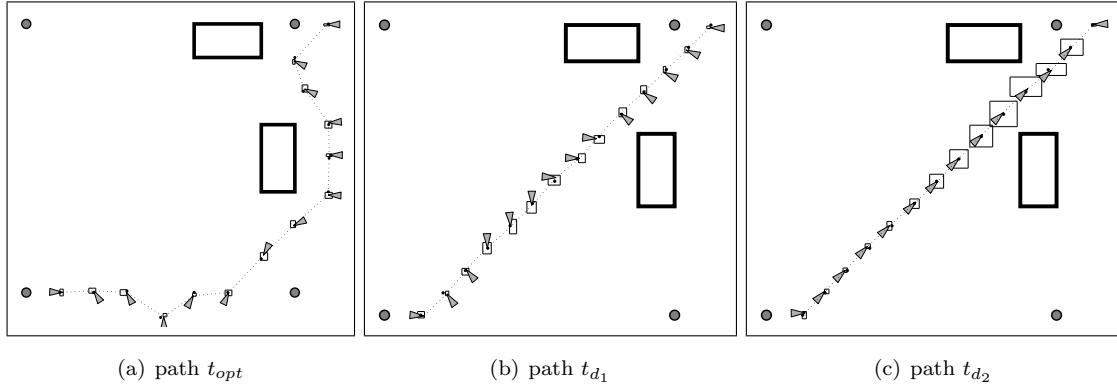


Figure 6: Scenario A with obstacles (thick boxes): comparison of localization uncertainty along three different paths. Gray disks indicate the landmarks, thin boxes represent the uncertainty on the robot position, triangles correspond to the true robot pose.

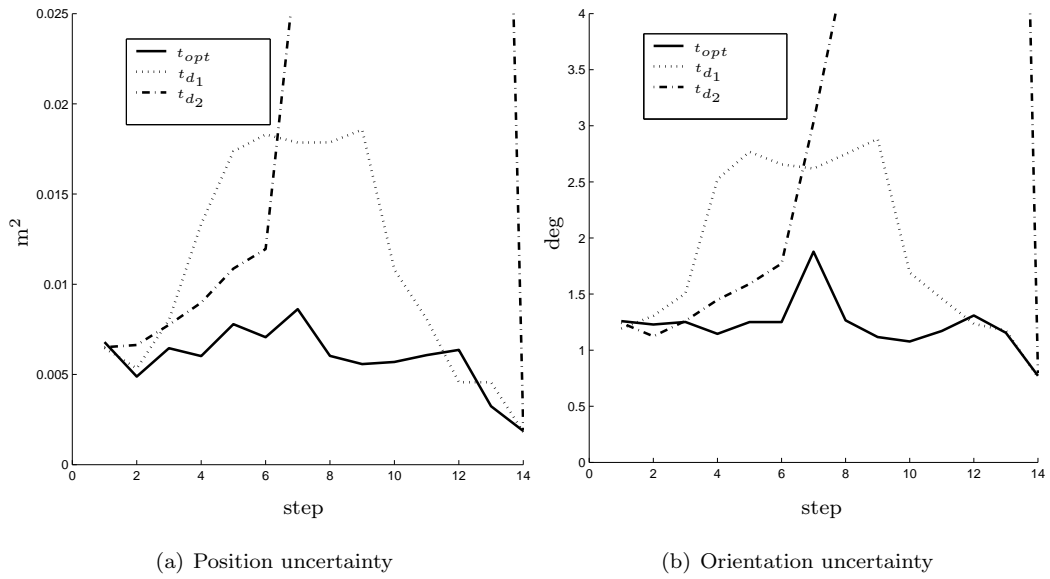


Figure 7: Scenario A with obstacles: (a) area of uncertainty boxes, (b) width of orientation intervals. Results are averaged over 100 simulation runs, for each of the three paths of Figure 6.

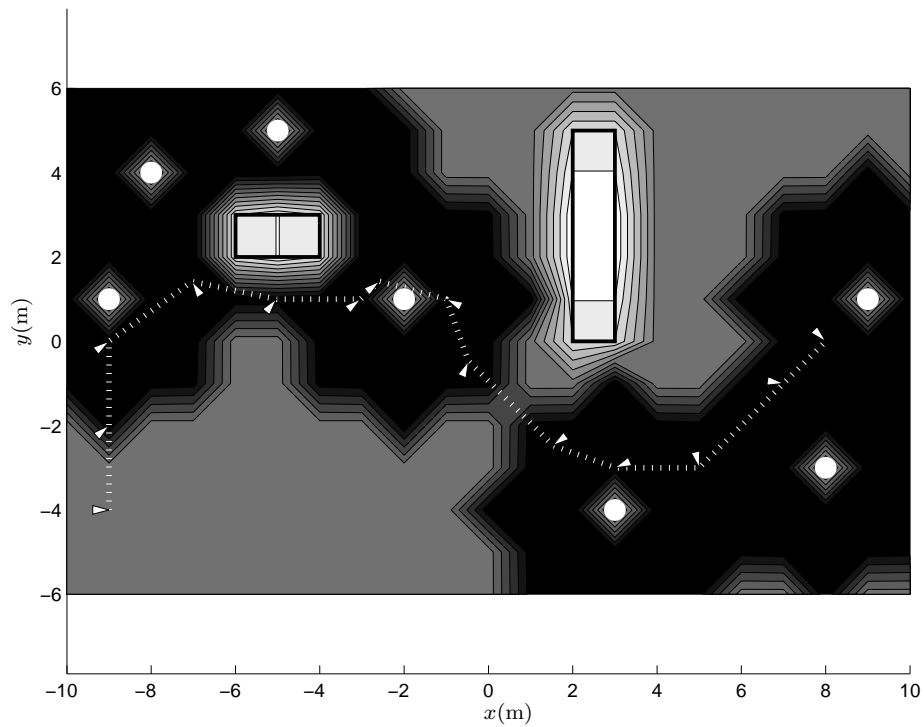


Figure 8: Scenario B: cost function (25) and optimal path.

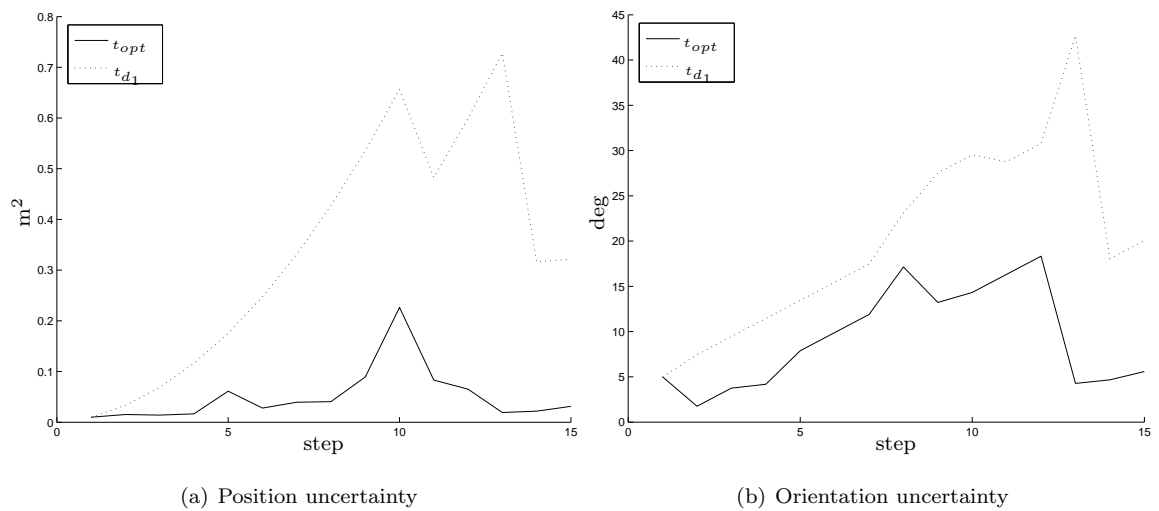


Figure 9: Scenario B: (a) area of uncertainty boxes, (b) width of orientation intervals during a run of the localization algorithm, along the optimal path (solid line) and the direct path with optimal orientation (dotted line).

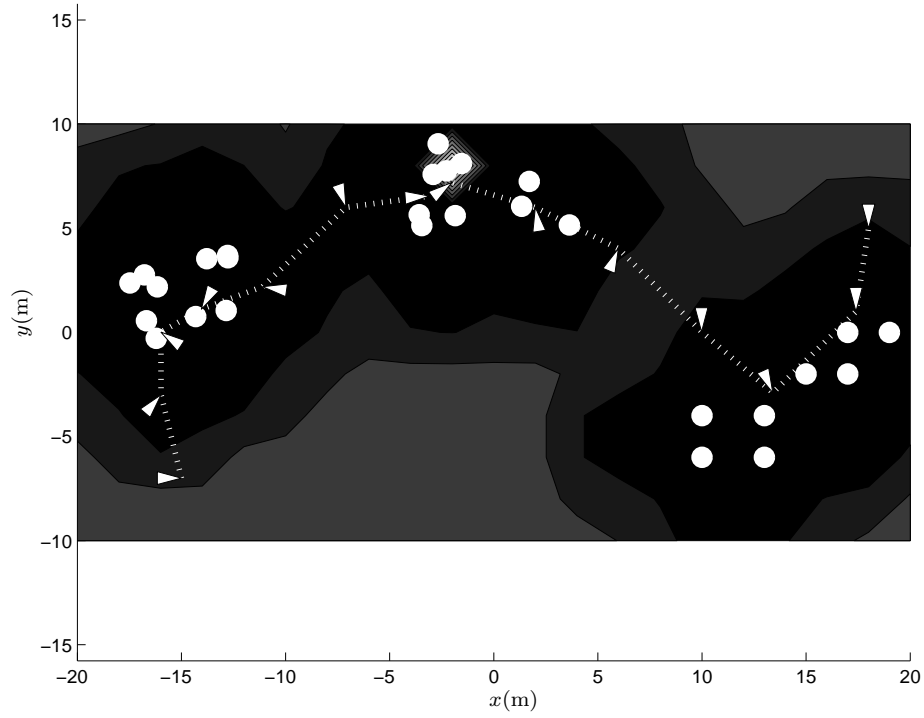


Figure 10: Scenario C: cost function (22) and optimal path.

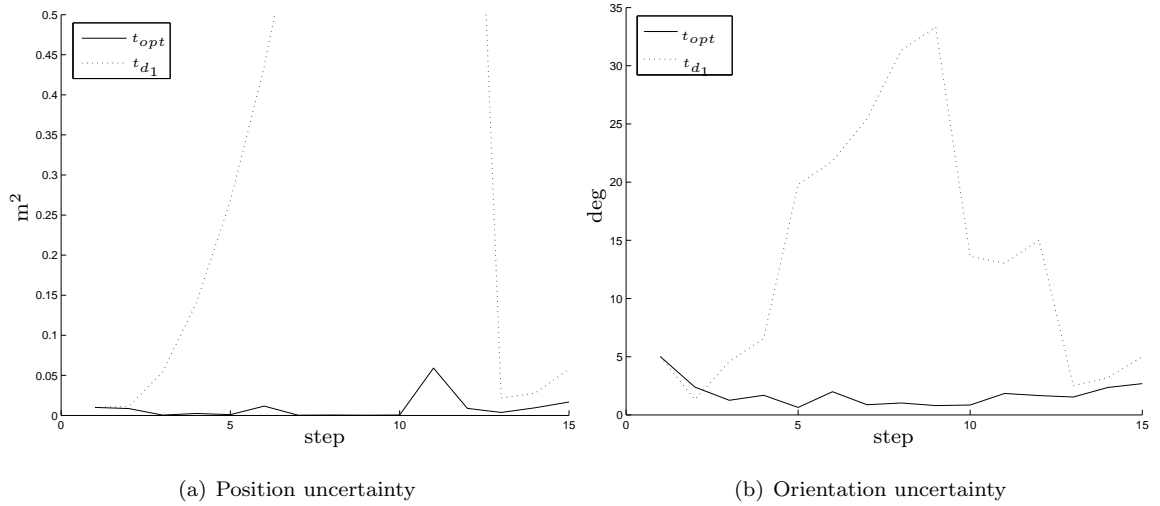


Figure 11: Scenario C: (a) area of uncertainty boxes, (b) width of orientation intervals during a run of the localization algorithm, along the optimal path (solid line) and the direct path with optimal orientation (dotted line).

5 CONCLUSIONS

A path planning algorithm which minimizes the localization uncertainty affecting the robot along the travelled path has been proposed. A deterministic description of the uncertainty has been adopted, leading to set-valued pose estimates whose size concurs to the definition of a suitable potential function to be minimized. Limited sensory range and obstacle avoidance are naturally accounted for in the considered problem formulation.

Although the considered scenario has been kept deliberately simple, in order to illustrate the main idea, several developments can be foreseen. More realistic motion models, including for example nonholonomic constraints or bounded odometric errors, can be incorporated. Different types of sensors and measurement models can also be treated. More efficient computational methods for tackling the resulting optimization problem and able to deal with discontinuous and/or disconnected solution sets should also be considered.

Along the road towards the integration of different tasks, such as localization, map building and path planning, within a fully autonomous navigation system, a challenging objective to be pursued is path planning within an environment which is unknown or only partially known. In this scenario, the uncertainty associated to each robot pose has to be evaluated by solving a SLAM problem, and the planner has to update the cost function in real-time according to the new information available in the map. This calls for further research involving both new techniques for uncertainty estimation and efficient methods for computing the objective function to be optimized.

References

- [1] M. Milanese and A. Vicino. Optimal estimation theory for dynamic systems with set membership uncertainty: an overview. *Automatica*, 27(6):997–1009, 1991.
- [2] M. Milanese, J. P. Norton, H. Piet-Lahanier, and E. Walter, editors. *Bounding Approaches to System Identification*. Plenum Press, New York, 1996.
- [3] S. Atiya and G. D. Hager. Real-time vision-based robot localization. *IEEE Transactions on Robotics and Automation*, 9(6):785–800, 1993.
- [4] A. Garulli and A. Vicino. Set membership localization of mobile robots via angle measurements. *IEEE Transactions on Robotics and Automation*, 17(4):450–463, August 2001.

- [5] L. Jaulin, M. Kieffer, E. Walter, and D. Meizel. Guaranteed robust nonlinear estimation with application to robot localization. *IEEE Transactions on Systems, Man, and Cybernetics, Part C: Applications and Reviews*, 32(4):374–381, November 2002.
- [6] K. Briechle and U. D. Hanebeck. Localization of a mobile robot using relative bearing measurements. *IEEE Transactions on Robotics and Automation*, 20(1):36–44, 2004.
- [7] A. Clerentin, M. Delafosse, L. Delahoche, B. Marhic, and A. Jolly-Desodt. Uncertainty and imprecision modeling for the mobile robot localization problem. *Autonomous Robots*, 24(3):267–283, April 2008.
- [8] M. Di Marco, A. Garulli, A. Giannitrapani, and A. Vicino. A set theoretic approach to dynamic robot localization and mapping. *Autonomous Robots*, 16:23–47, January 2004.
- [9] L. Jaulin. A nonlinear set membership approach for the localization and map building of underwater robots. *IEEE Transactions on Robotics*, 25(1):88–98, February 2009.
- [10] M. Di Marco, A. Garulli, A. Giannitrapani, and A. Vicino. Simultaneous localization and map building for a team of cooperating robots: a set membership approach. *IEEE Transactions on Robotics and Automation*, 19(2):238–249, 2003.
- [11] J. Reif. Complexity of the mover’s problem and generalizations. In *Proceedings of the 20th IEEE Symposium on Foundations of Computer Science*, pages 224–241, 1979.
- [12] J.C. Latombe. *Robot Motion Planning*. Kluwer Academic Publishers, 1991.
- [13] H. Takeda, C. Facchinetti, and J. C. Latombe. Planning the motions of a mobile robot in a sensory uncertainty field. *IEEE Transactions on Pattern Analysis and Machine Intelligence*, 16(10):1002–1017, October 1994.
- [14] A. Lambert and Th. Fraichard. Landmark-based safe path planning for car like robots. In *Proceedings of the IEEE International Conference on Robotics and Automation*, pages 2046–2051, San Francisco, CA, 2000.
- [15] A. Lambert and D. Gruyer. Safe path planning in an uncertain-configuration space. In *Proceedings of the IEEE International Conference on Robotics and Automation*, volume 3, pages 4185–4190, September 2003.
- [16] L. Blackmore, H. Li, and B. Williams. A probabilistic approach to optimal robust path planning with obstacles. In *Proceedings of the American Control Conference*, June 2006.

- [17] J. P. Gonzalez and A. T. Stentz. Planning with uncertainty in position using high-resolution maps. In *Proceedings of the IEEE International Conference on Robotics and Automation*, pages 1015–1022, Roma, April 2007.
- [18] A. Lazanas and J.C. Latombe. Motion planning with uncertainty: a landmark approach. *Artificial Intelligence*, 76:287–317, 1995.
- [19] L. A. Page and A. C. Sanderson. Robot motion planning for sensor-based control with uncertainties. In *Proceedings of the IEEE International Conference on Robotics and Automation*, volume 2, pages 1333–1340, Nagoya, May 1995.
- [20] M. E. Campbell and J. Ousingawat. On-line estimation and path planning for multiple vehicles in an uncertain environment. In *Proceedings of the AIAA Guidance, Navigational and Control Conference*, 2002.
- [21] N. Ceccarelli, M. Di Marco, A. Garulli, and A. Giannitrapani. A set theoretic approach to path planning for mobile robots. In *IEEE Conference on Decision and Control*, pages 147–152, Atlantis, Bahamas, December 2004.
- [22] Z. Shiller and S. Dubowsky. Global time optimal motions of robotic manipulators in the presence of obstacles. In *Proceedings of the IEEE Conference on Robotics and Automation*, pages 370–375, Philadelphia, PA, April 1988.
- [23] J. Guivant and E. Nebot. Optimization of the simultaneous localization and map-building algorithm for real-time implementation. *IEEE Transactions on Robotics and Automation*, 17(3):242–257, 2001.